Environmental Science & Technology

Article

Cite This: Environ. Sci. Technol. 2019, 53, 2570−2578

pubs.acs.org/est

Updated Hourly Emissions Factors for Chinese Power Plants Showing the Impact of Widespread Ultralow Emissions Technology Deployment

Xiao Liu,[†] Xing Gao,[†] Xinbin Wu,[‡] Weilin Yu,[†] Lulu Chen,[§] Ruijing Ni,[§] Yu Zhao,[∥] Hongwei Duan,[‡] Fuming Zhao,[‡] Lilin Chen,[‡] Shengming Gao,[‡] Ke Xu,[†] Jintai Lin,*[,§] and Anthony Y. Ku*[,†,⊥]

[†]National Institute of Clean-and-Low-Carbon Energy, Beijing 102211, China

[‡]Shenhua Environment Remote Sensing and Monitoring Center, Shenhua Geological Exploration Company, Beijing 102211, China

[§]Laboratory for Climate and Ocean-Atmosphere Studies, Department of Atmospheric and Oceanic Sciences, School of Physics, Peking University, Beijing 100871, China

[∥]State Key Laboratory of Pollution Control & Resource Reuse and School of the Environment, Nanjing University, 163 Xianlin Avenue, Nanjing, Jiangsu 210023, China

[⊥]NICE America Research, 2091 Stierlin Ct, Mountain View, California 94043, United States

Supporting Information

ABSTRACT: Nationwide severe air pollution has prompted China to mandate the adoption of ultralow emissions (ULE) control technologies at all of its coal-fired power plants by 2020. This process has accelerated greatly since 2014 and, combined with operational adjustments related to overcapacity, has reduced the emissions of nitrogen oxides (NO_x), sulfur dioxide (SO_2), and particulate matter (PM). Yet the quantitative understanding of ULE benefits is poor. Using detailed emissions data from 38 units at 17 power plants, corresponding to 10 combinations of ULE technologies representative of the Chinese power sector, we show that emissions factors for NO_x, SO_2, and PM are up to 1−2 orders of magnitude lower after ULE retrofitting. The effectiveness in cutting emissions shows a large spread across the various ULE technology combinations, providing an opportunity to choose the most efficient, economically viable technology (or a combination of technologies) in the future. The temporal variations in emissions at hourly resolution reveal the effects of power plant load on emissions, an increasingly important factor given that power plants are not operated at full capacity. These data will be useful in efforts to understand the evolving state of air quality in China and can also provide a basis for benchmarking state-of-the-art air pollution control equipment globally.

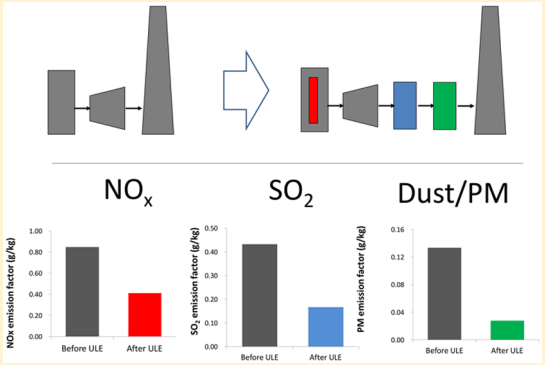

INTRODUCTION

The Chinese government has implemented a number of measures to reduce ambient air pollution,[1] particularly by cutting emissions in the coal-fired power sector. In particular, power companies in China are required to install suites of "ultra-low emissions" (ULE) technologies that can reduce nitrogen oxides (NO_x), sulfur dioxide (SO_2), and particulate matter (PM, including particles of all sizes) emissions from coal-fired power plants to levels comparable to emissions standards for natural gas-fired power plants. Retrofitting with ULE technologies began in 2014 and is expected to cover around 90% of coal-fired power plants in China by the end of 2020.[2] (See Supporting Information, S1 for details on the ULE implementation requirements.) The net effect of these policies has been a significant and accelerating reduction in emissions from coal power plants over the past few years.

Implementation of ULE technologies may have altered the characteristics of power plant emissions beyond a change in the mean value, with important implications for modeling and understanding the effectiveness in reducing ambient pollution. Early studies of power sector emissions in China computed total emissions from annual statistics for regional coal consumption using averaged emissions factors (EFs).[3] Subsequent inventories have improved upon the spatial resolution and accuracy through the incorporation of data at the power plant level.[4−7] The most comprehensive unit-based inventory is the China Coal-Fired Power plant Emissions Database (CPED), which reports emissions and EF values up to 2010.[8] Data for some new advanced reduction technologies

Received: December 22, 2018
Accepted: January 28, 2019
Published: January 28, 2019

DOI: 10.1021/acs.est.8b07241
Environ. Sci. Technol. 2019, 53, 2570−2578

have been reported recently.[9−12] However, a more comprehensive emissions assessment for plants equipped with a full-suite of ULE technologies has not yet been published. For example, ULE technologies may offer benefits beyond those provided by individual technologies; e.g., flue gas desulfurization (FGD) systems appear to offer additional minor benefits in the control of NO_x and PM.[13,14] In addition, the performance of emissions control equipment greatly depends on the specific configuration, as shown in this study.

How ULE technologies may have altered the temporal variability of emissions is also an important question. Since most haze episodes build up within hours,[15,16] accurate atmospheric modeling requires emissions data with resolution on this time scale.[8,17] Most published emissions inventories report monthly profiles. Although some inventories provide hourly profiles, these profiles do not change from one day to another or from one region to another.[8,18] One driver for hourly variations is load-cycling at power plants in China. Overcapacity in the power sector has steadily reduced the capacity factor of the power plant fleet, and this has led to some plants being operated in a dynamic manner. Load-cycling can increase the complexity of the interactions between emissions and haze formation.[19] In addition, turndown of power plants can reduce the thermal efficiency of the plant, resulting in higher coal consumption and higher emissions for a given amount of power output. To date, the effects of load on EF and removal efficiencies are poorly documented, and initial data at Chinese power plants indicate that the relationship between these parameters (EF and removal efficiencies) and load, while monotonic, may not be linear.[9,19,20] Updated EF based on higher frequency data is the most direct way to address limitations in temporal resolution. This approach is used in the United States and other countries.[21−24] However, emissions inventories at this level of temporal resolution have not yet been developed for Chinese coal-fired power plants.

On the basis of detailed information from China Energy Group, the largest coal power company in the world, we analyze the variability of hourly emissions and EF of NO_x, SO_2, and PM during 2015−2017 across different power-generating units, ULE technology configurations, loads, and time. Data were collected from 38 units at 17 coal-fired power plants retrofitted with ULE technologies between 2014 and 2016. Our data set includes power plants with steam turbine rated capacities from 215 to 1050 MW; power plants with this capacity range represent about 80% of the total capacity in China in 2015.[25] The ULE technologies and technology configurations examined here represent all possible cases for pulverized coal (PC) boilers; together, these PC boilers provide more than 95% of coal-fired capacity, with the rest of the capacity being provided by circulating fluidized bed (CFB) boilers. High frequency data in intervals of seconds to 1 h are available for flue gas flow rate, pollutant mass concentrations in the flue gas, power load, and other ancillary parameters, allowing, to our knowledge, the first estimate of unit-resolved hourly emissions and EF for power plants in China equipped with ULE technologies.

DATA AND METHODS

Power Generation Units and ULE Technologies. In this paper, ULE technologies refer to a variety of individual emissions control technologies for NO_x, SO_2, and PM removal.[10] ULE technologies also can include upgrading of existing emissions controls through new hardware or optimization of existing equipment. As listed in Supporting Information Table S1, the current national standards[26] require that for a power unit to claim "ULE", its emissions levels must not exceed 50, 35, and 5 mg per cubic meter as at the standard state (at 1 atm and 273.15 K) (mg/m^3) for NO_x, SO_2, and PM mass concentrations in the flue gas.

Supporting Information S2 presents the 38 units from 17 power plants considered for this study, their geographical locations, nameplate generation capacity, emissions control technologies, and the date ULE technologies were installed at the plant (Supporting Information, Table S2 and Figure S1). Plants are grouped by geographic region and type (i.e., with or without heat cogeneration). Eighteen power-only units and 20 electricity and heat cogeneration units are considered. The equipment for 10 distinct configurations for ULE technologies at power units surveyed here are representative of the situation across the Chinese power sector. Specific technologies include low NO_x burner (LNB) and selective catalytic reduction (SCR) for NO_x control; seawater flue gas desulfurization (SFGD), limestone-gypsum wet flue gas desulfurization (WFGD), and an emerging technology (SPC) for SO_2 control; and dry electrostatic precipitator (ESP), low-low temperature electrostatic precipitator (LLT-ESP), wet electrostatic precipitators (WESP), WFGD, SFGD, and SPC for PM control. A technical description of the SPC technology can be found in the Supporting Information.

Data Collection for Emissions Factors Calculation. Data for 38 units from January 2015 through October 2017 were used to calculate the EFs. The data were downloaded from the Continuous Emission Monitoring System (CEMS) database developed by China Energy Group (Supporting Information S2). In 25 units in 12 plants, ULE technologies were introduced during the sampling period, and thus paired data sets from before and after retrofitting of ULE technologies were available for comparison. These data were used to explore the impact of ULE retrofit routes at individual units. The remaining 13 units in 5 plants were retrofitted before the data sampling period, and their data were used to facilitate the analysis of post-ULE EFs.

Depending on type, high frequency data, daily data, or annual data were available. High frequency data measured at each unit at intervals of 5−25 s were available for NO_x, SO_2, and PM concentrations in the flue gas as well as flue gas volume flow rate. Supporting Information Table S3 reports details for specific measurement methods. The flow rate and pollution concentration data used here were measured with rigorous validation procedures to ensure data quality (see details in Supporting Information S3). These data were corrected to the standard state using measured temperature and pressure in the flue gas and recorded in the CEMS. Power generation data, also at intervals of 5−25 s, are available for 18 electricity-only units.

Daily reported data include the generated standard vapor, raw coal consumption rate, and sulfur content in coal. Other coal properties such as the ash content in coal, and the lower heating value were recorded less frequently, and their annual average values in 2016 were used in this study. The sulfur and ash contents varied with time and location, and their annual average values are shown in Supporting Information Table S4.

Derivation of Emissions and Emissions Factors. Emissions (g/s) are the product of flue gas volume flow rate (m^3/h), pollutant concentrations (mg/m^3), and a scaling factor for unit conversion (0.001 g/mg). Daily emissions factors and

DOI: 10.1021/acs.est.8b07241
Environ. Sci. Technol. 2019, 53, 2570−2578

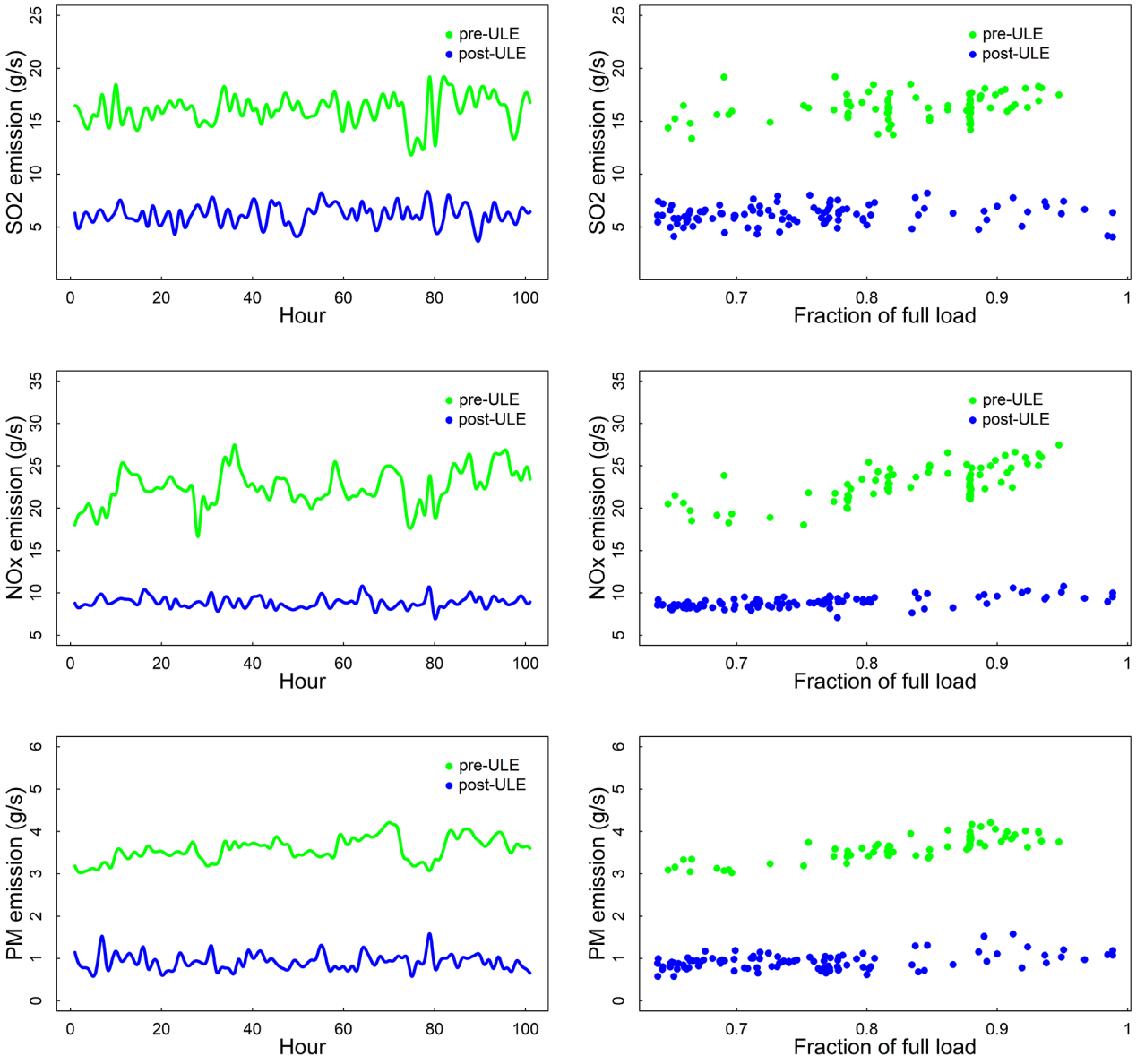

Figure 1. (Left) Hourly emissions over 100 consecutive hours before and after ULE retrofit at an electricity-only unit, JH1. (Right) Respective emission results as a function of relative electricity load. All data are provided in the Supporting Information, Data File (Sheet name: Figure 1).

hourly emissions factors were calculated using the same way—by dividing the emissions by the coal consumption over the period of interest.

Daily EFs were calculated for all 38 units. Here, daily EFs were calculated as daily emissions divided by daily standard coal consumption. The amount of daily standard coal consumption was calculated from daily raw coal consumption and the annual average lower heating value at each unit:

$$W_S = W_R \times Q_L/Q_S \quad (1)$$

where Q_S is the lower heating value for standard coal (29307.6 J/kg), Q_L is lower heating value for the raw consumed coal, W_S is the standard coal consumption by mass, and W_R is the raw coal consumption by mass recorded each day for the given unit.

Hourly EFs were calculated for the 18 electricity-only units, as emissions in an hour divided by coal consumption in that hour. Hourly emissions were calculated from contiguous blocks of high frequency flow rate and pollutant concentration data that span at least 45 min in a given hour. Since hourly coal consumption data were not directly available, the hourly electrical output was used to help estimate the hourly coal consumption for these 18 units. For each day, the daily standard coal consumption was assigned to each hour according to the fraction of hourly electricity output (i.e., power load) in the daily total electricity output. We removed outliers in hourly EF data by excluding values below 2.5 percentile or above 97.5 percentile; these outliers were caused by a variety of operational issues that we do not intend to address here. The daily average of hourly EF values are similar to the daily EFs calculated based on daily emissions (see Supporting Information, Data File "Hourly & daily mean and STD").

DOI: 10.1021/acs.est.8b07241
Environ. Sci. Technol. 2019, 53, 2570−2578

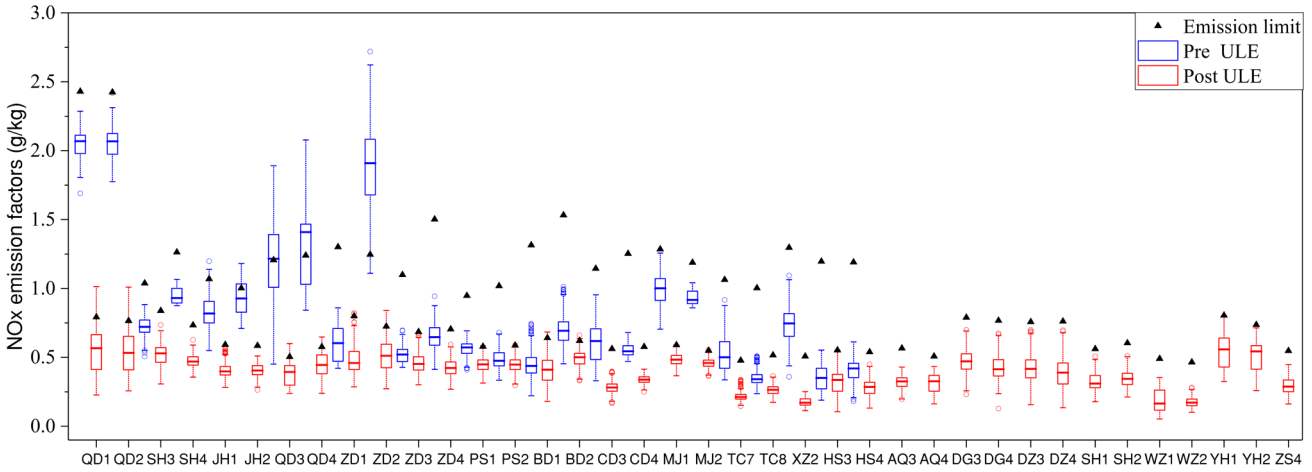

Figure 2. Box plots for NO_x emissions factors before (blue) and after (red) ULE retrofit at 38 units. The thick horizontal line inside each box represents the mean over the sampling period, the height of the box denotes one standard deviation, and the dashed vertical line denotes the confidence level at the 95% level. The black filled triangles represent the regulatory EF limits for before ULE (blue) and ULE (red). The 13 units on the right finished ULE retrofitting before the study period. All data are provided in the Supporting Information Data File (Sheet name: Figures 2−4).

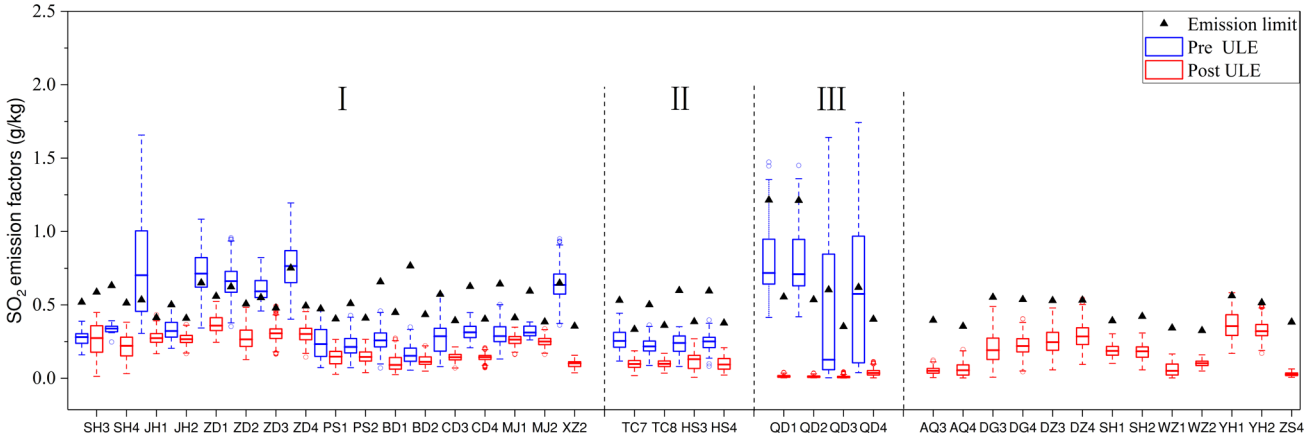

Figure 3. Box plots for SO_2 emissions factors before (blue) and after (red) ULE installation at 38 units. The thick horizontal line inside each box represents the mean over the sampling period, the height of the box denotes one standard deviation, and the dashed vertical line denotes the confidence level at the 95% level. Power plant units in group I equipped WFGD technology, II with SPC, and III with SFGD. The 13 units on the right finished ULE retrofitting before the study period. The black filled triangles represent the regulatory EF limits. All data are provided in the Supporting Information Data File (Sheet name: Figures 2−4).

RESULTS

Hourly Emissions at an Exemplary Unit in Actual Operation. The left panels of Figure 1 show hourly emissions of NO_x, SO_2, and PM over 100 consecutive hours before (green lines) and after (blue lines) retrofitting with ULE technologies at an exemplary electricity-only unit, JH1. At this unit, LNB and SCR were used to achieve ULE for NO_x, WFGD for SO_2, and LLT ESP, WFGD, and WESP for PM. For these pollutants, emissions are reduced by a factor of 2−5 after retrofitting, reflecting the effectiveness of ULE technologies in actual operation. Also, there is significant hour-to-hour and day-to-day variations with no obvious cycles, reflecting the complexity in the actual power plant emissions that is not taken into account in air quality modeling studies.

The right panels of Figure 1 show the dependence of pollutant emissions on relative power load (as fraction of full capacity) at times consistent with the left panels. Before retrofitting with ULE technologies, emissions increased with increasing load, although there is large scatter in emissions. The growth and scatter in emissions are much reduced after retrofitting, in addition to a reduction in the mean values. These changes reflect the complex influences of ULE implementation on emission properties beyond a reduction in the mean EF.

Effects of Retrofitting with ULE Technologies on Emissions Factors. The box plots in Figures 2−4 show the variation of EFs across power units before (left panels) and after (right panels) retrofitting with ULE technologies for each pollutant. Results are presented for the 25 units for which retrofitting occurred during our sampling period and an additional 13 units where retrofitting was completed before the data sampling period. The regulatory limits for EFs, which were calculated with emissions concentration limits (100, 50, and 20 mg/m^3 for NO_x, SO_2, and PM, respectively, before ULE; and 50, 35, and 5 mg/m^3 after ULE), flue gas volume, and coal consumption, are also shown as black triangles.

As listed in Supporting Information Table S5 for the variety of ULE retrofit routes for the 25 units, most of sampled units already had some pollution control equipment. In these cases,

DOI: 10.1021/acs.est.8b07241
Environ. Sci. Technol. 2019, 53, 2570−2578

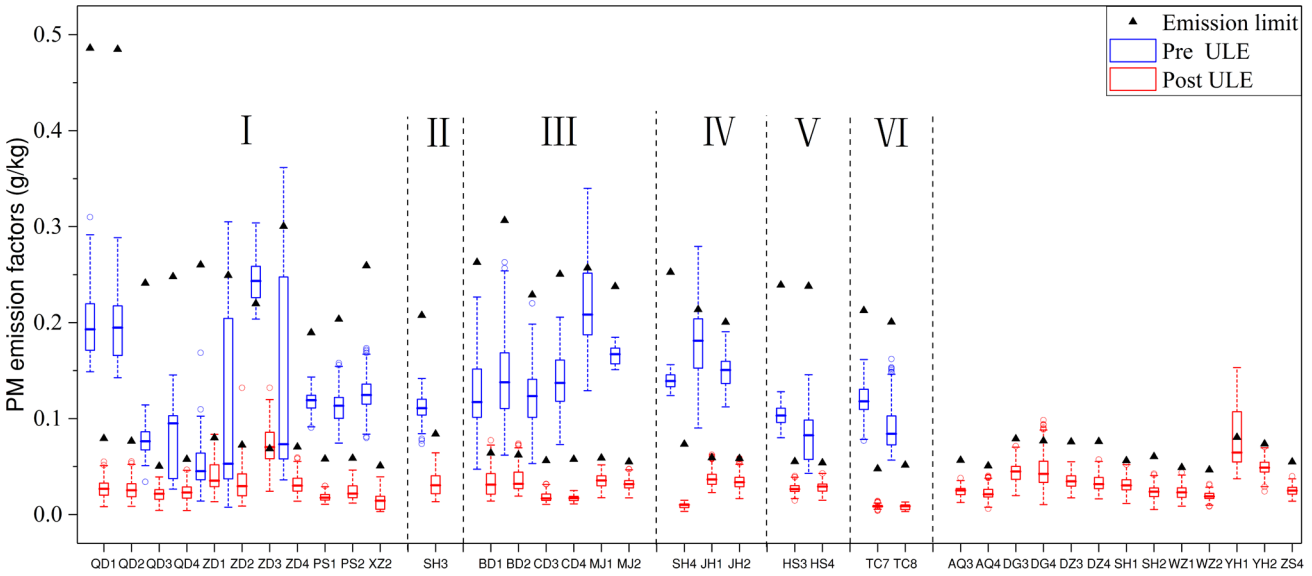

Figure 4. Box plots for PM emissions factors before (left) and after (right) ULE installation at 38 units. The thick horizontal line inside each box represents the mean over the sampling period, the height of the box denotes one standard deviation, and the dashed vertical line denotes the confidence level at the 95% level. Power plant units in group I equipped ESP + WFGD/SFGD, II with ESP + WFGD/SFGD + WESP, III with LLT ESP + WFGD, IV with LLT ESP + WFGD + WESP, V with SPC, and VI with LLT ESP + SPC + WESP. The 13 units on the right finished ULE retrofitting before the study period. The black filled triangles represent the regulatory EF limits. All data are provided in the Supporting Information Data File (Sheet name: Figures 2–4).

retrofitting with ULE technologies involved upgrading previous equipment and installing new reduction equipment.

Effect on NO_x Removal. Figure 2 shows substantial variability in NO_x EFs across the 25 units before ULE retrofit. The temporally averaged EF at each unit varied by a factor of 6, from 0.35 to 2.05 g/kg, with a mean value of 0.85 g/kg. After retrofitting with ULE technologies, the temporal and cross-unit mean EF declined to 0.41 g/kg, and the cross-unit variability is also reduced to 0.17–0.55 g/kg. The mean EF value after retrofitting (0.41 g/kg) was equal to 33.9 ± 7.6 mg/m^3 in terms of pollutant concentration in the flue gas, in compliance with the ULE regulatory standard of 50 mg/m^3. The reduction in NO_x EFs after retrofit was smaller than for SO_2 and PM (see below), because before ULE retrofit the power units were already equipped with SCR and (in some cases) LNB to reduce NO_x emissions, and the retrofit process was primarily focused on optimization of the existing equipment rather than installing new hardware.

Effect on SO_2 Removal. Figure 3 compares the SO_2 EFs before and after retrofitting with ULE technologies at the 25 units. Across the units, retrofitting reduced the temporal mean EF value from 0.16–0.81 g/kg (0.43 g/kg on average) to 0.01–0.37 g/kg (0.17 g/kg on average). The postretrofit temporal and cross-unit average EF (0.17 g/kg) was equivalent to 13.3 ± 7.0 mg/m^3 in the flue gas, in compliance with the ULE regulatory standard of 35 mg/m^3. At four units (ZD1, ZD2, ZD3, and ZD4), the pre-ULE temporal average EF exceed the regulatory pre-ULE limits, whereas the post-ULE EFs are below the ULE regulatory limits, even though the pre-ULE limits are higher than the ULE limits.

Among the three control technologies (SFGD, SPC, and WFGD), SFGD results in the lowest EF (0.018 g/kg on average). An important advantage of SFGD is the use of inexpensive seawater. The high removal efficiency was due, in large part, to the use of large amounts of circulating seawater to maintain sulfur removal efficiency no less than 98%. At units equipped with WFGD, the retrofitting process is focused on optimization of flow distribution in existing equipment; as such, the resulting EF reduction is not as large as those for units lacking effective emission control prior to retrofit.

The SO_2 concentration in the flue gas before passing the emissions control equipment depends on the sulfur content in coal. The sulfur content in the 25 units varied by up to a factor of 3, from 0.3% to 0.8%. To ensure low SO_2 emissions after the pollutant removal process, ULE technologies for units burning higher-sulfur coal must maintain higher removal efficiencies. Supporting Information Figure S2 plots the daily EF and removal efficiency for SO_2 as a function of daily sulfur content in the coal consumed cross 25 units. The figure shows weak dependence of post-ULE EF on the sulfur content (left panel) because of the higher removal efficiency (right panel), for all three control technologies (SFGD, SPC, and WFGD).

Effect on PM Removal. Figure 4 shows that after retrofitting with ULE technologies, the temporal mean EF of PM were reduced from 0.08–0.25 g/kg across the 25 units (0.13 g/kg on average) to 0.01–0.07 g/kg (0.03 g/kg on average). This substantial reduction is not surprising given the emphasis of air pollution control policies on PM removal. The post-ULE EF (0.03 g/kg) was equivalent to 2.3 ± 1.0 mg/m^3 in the flue gas, in compliance with the ULE standard of 5 mg/m^3. ULE retrofitting also reduces the temporal variability of EFs greatly. We found no clear evidence of any superiority among the six ULE configurations in EF reduction.

Effects of ULE Retrofit Routes on Emissions Factors. The retrofitting of ULE technologies involved a combination of installing new equipment and improving existing equipment. This section examines the effect of different technology pathways for ULE retrofitting. Among the 25 units, there were four distinct retrofitting routes for NO_x removal, four for SO_2, and six for PM.

Figure 5 plots the ratio of the average EF before and after retrofit for each of the technology routes. For NO_x, the ratio

DOI: 10.1021/acs.est.8b07241
Environ. Sci. Technol. 2019, 53, 2570–2578

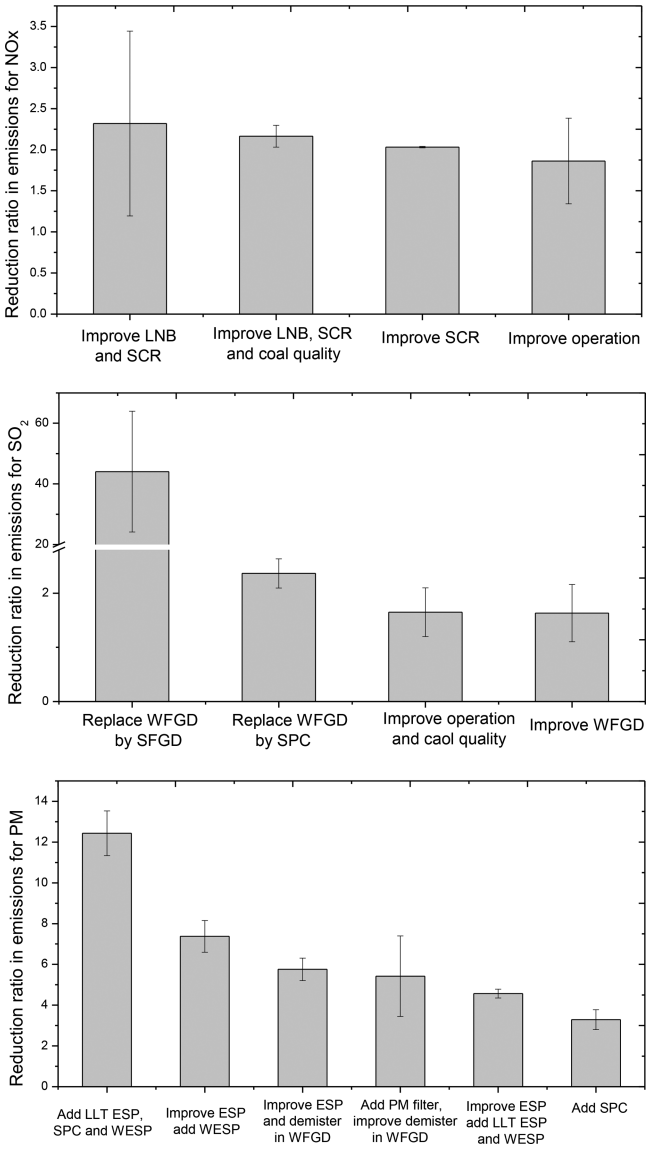

Figure 5. Ratio of EFs before and after ULE retrofit for each route of ULE retrofit, averaged over all units with the same route of ULE retrofit. Error bars represent one standard deviation. All data are provided in the Supporting Information Data File (Sheet name: Figure 5).

ranged from about 2−2.5 across the four routes, with the unit-to-unit variability illustrated by the error bars. For SO_2, replacing WFGD by SFGD reduced the EF by a factor of about 45; the other three routes only reduced the EF by a factor of about two. For PM, the pre-ULE to post-ULE EF ratio varied from 3.3 to 12.5 across the six routes, indicating a wider spread in the effectiveness of various technology configurations. Despite this variation, the ULE technologies brought the pollutant emissions into compliance with regulatory requirements for all of the plants surveyed in this study. Put another way, power units that had relatively high emissions before retrofitting with ULE technologies experiencing greater improvement.

Diurnal Variability in Post-ULE Emissions Factors and Dependence on Power Load. Figure 6 shows the diurnal variation of power load and pollutant EFs after retrofitting with ULE technologies. Results are presented for the 18 electricity-only units with hourly load data. The time is expressed in Beijing Standard Time. Two units, YH1 and YH2, are located in Yinchuan with about 1 h lag in local solar time relative to Beijing; we thus shifted the data at these two units by 1 h to synchronize the data. At each hour, 95% CI of load or EF was averaged over all days at each unit and then over all units, and the error bar in Figure 6 represents the standard deviation across the 18 units.

The relative load data shows a weak diurnal pattern, with two peaks consistent with socioeconomic activities. The first peak occurs before noon time, which is likely associated with intensified commercial activity and consequent electricity consumption. The second peak occurs around dinner time. The load reaches a minimum around 4:00 am due to reduced residential and industrial power demand. The daytime peaks are similarly about 20% larger than the nighttime minimum. There was large scatter of load in any given hour, illustrating the need to be careful about drawing too many conclusions about patterns from the data without deeper analysis into the drivers behind power demand at individual sites.

Figure 6 shows that for all three pollutants, the average post-ULE EF shows a very weak diurnal pattern. Although there is slight diurnal variability, such variability is insignificant compared to the large variability across the units. The apparently weak correlation between EF and boiler load is consistent with the expectation that the emission performance is decoupled from the boiler operation.

Day-to-Day and Cross-Unit Variability in Post-ULE Emissions Factors. Figure 7 shows the frequency distribution of daily mean post-ULE EF across all days and all 38 units for each pollutant, together with the sulfur content of consumed coal. For NO_x, the frequency distribution appears to be Gaussian, with a peak around the EF value of 0.48 g/kg. For SO_2, there are clearly three peaks in the frequency around EF values of 0.02, 0.15, and 0.27 g/kg, respectively, representing the distinctive effects of three ULE configurations (SFGD, SPC, and WFGD). For PM, the frequency distribution of EFs largely follows the Weibull distribution with a peak frequency at the EF value of 0.03 g/kg, as a combined effect of the six ULE configurations.

Zhao et al. have also attempted to establish statistical distributions of EFs as a way to quantify the variability across a fleet of power plants and to present measurement errors.[5] Using data from an unpublished government survey, they estimated the removal efficiency of WFGD in practice to be 75% on average, with a triangular distribution (from 55% to 95%). The effects of other FGD systems were estimated to be poorer, with an average removal efficiency of only 20%[5] and a triangular distribution (from 10% to 60%). Our SO_2 EF data do not show such triangular distributions (Figure 7). Zhao et al. also used data from field measurements to quantify the performance of ESP,[5] and found removal efficiencies for $PM_{2.5}$, $PM_{2.5-10}$, and PM_{10} of 92.31%, 96.97%, and 99.46% with log-normal, log-normal, and normal distributions, respectively. The shapes of these normal or log-normal distributions are similar but different from the Weibull distribution shown in our PM EF data. Further studies are warranted to address the causes in actual operation of these various distributions.

DISCUSSION

Comparison of Our Post-ULE Emissions Factors with the Literature. We further compare our post-ULE EF results (averaged over all 38 units) with those in the literature for Chinese power plant emissions. Overall, our post-ULE EF are

DOI: 10.1021/acs.est.8b07241
Environ. Sci. Technol. 2019, 53, 2570−2578

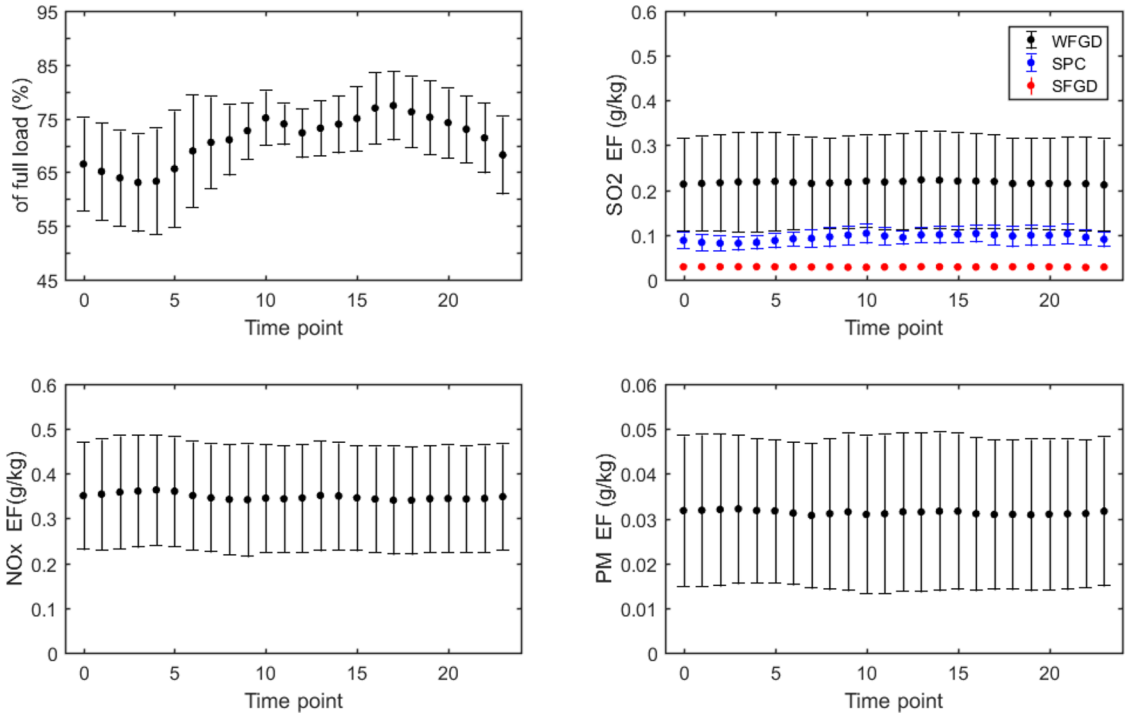

Figure 6. Diurnal cycle of power load and EFs averaged over all days, for the 18 electricity-only units with available hourly load data. Error bars represent one standard deviation across the units. All data are provided in the Supporting Information Data File (Sheet name: Figure 6).

lower than those in the literature, which represent years before 2017, by a factor of 8−23 for NO_x, 2−80 for SO_2, and 10−120 for PM. The magnitude of improvement depends on ULE configurations, among other factors. See Supporting Information S4 for detailed descriptions.

Implications. High frequency data over 2015−2017 from 38 power units within the China Energy Group fleet confirm that the widespread adoption of ULE technologies is substantially reducing emissions from coal-fired power plants across China. Our estimates of EFs after ULE retrofit for NO_x (0.48 ± 0.11 g/kg for mean and cross-unit standard deviation), SO_2 (0.02 ± 0.01, 0.1 ± 0.02 and 0.27 ± 0.09 g/kg for SFGD, SPC and WFGD, respectively), and PM (0.01 ± 00.05 to 0.01 g/kg, technology dependent) are lower than national fleet-averaged values from earlier years by up to 1−2 orders of magnitude. Although certain emissions control technologies had already been implemented before retrofitting, optimization of the existing systems still reduced the EF by a factor of 2 or more, as seen in paired data sets for individual units before and after ULE retrofit. The effectiveness of emission reduction shows a great spread among the ULE technologies and technology configurations. This increases the difficulty in understanding the effectiveness of current equipment in reducing pollution (especially on a local scale), but at the same time provides a basis for choosing the most economically viable and environmentally friendly technology (configuration) in the future.

The deployment of ULE technologies also reduces the scatter of EFs across time and units, although the cross-unit variation is still substantial. The EFs depend not only on the type of emission control technology but also on how various technologies are implemented or mixed in actual operation. Thus, using the regional/temporal average EF for a particular type of control technology to calculate emissions at smaller temporal or spatial scales may be subject to data-spread related uncertainty. The post-ULE EFs are insensitive to the power load, which shows a slight diurnal pattern consistent with local social and economic cycles. Future studies can extend this work to other power units and industrial boilers to better characterize the features of pollutant emissions.

The complex temporal and cross-unit variability both before and after retrofitting with ULE technologies shown here poses an important challenge for accurate air quality simulation and forecasting. Especially for air quality forecast in high temporal (i.e., hourly) and spatial (i.e., a few km^2) resolutions, a dynamic unit-based high frequency emission data set reflecting the actual power and industrial operations is needed. In this respect, our updated EFs represent an upgrade over the current emission inventories,[8,27,28] and are expected to improve the accuracy of atmospheric modeling.

A final point concerns the effect of economic incentives on emissions performance. Over the period studied, regional governments offered a subsidy of up to 1 cent RMB/kWh (2−3.3% of electricity grid price) for power plants complying with the ULE emissions standards. We noticed that the operation of emissions control technologies did not always follow the boiler operation (i.e., emissions control equipment was operated at 55−85% of full capacity even when the boiler was turned down to levels as low as 40%). We suspect that operating at this higher fraction of ULE control capacity was done to preserve sufficient margin to ensure continual compliance with ULE standards. It is quite possible that, as experience is gained, operators may choose to operate with less margin, resulting in a higher absolute emissions level, closer to the regulatory limit. This could result in a slight increase in EFs, as the performance converges to levels stipulated by regulation.

DOI: 10.1021/acs.est.8b07241
Environ. Sci. Technol. 2019, 53, 2570−2578

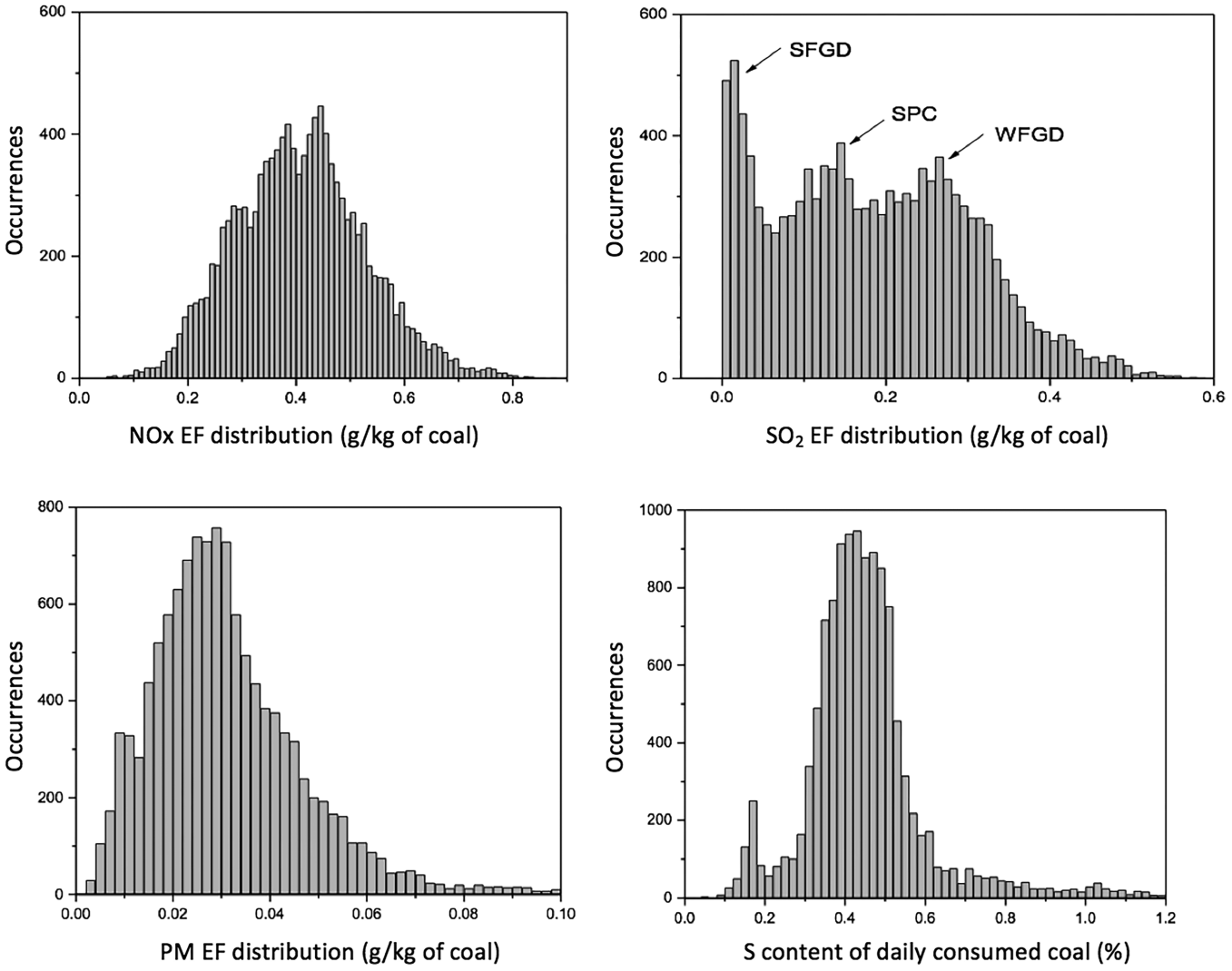

Figure 7. Frequency distribution of daily mean EF and S content from all days at the 38 sampled units. All data are provided in the Supporting Information Data File (Sheet name: Figure 7).

■ ASSOCIATED CONTENT

Supporting Information

The Supporting Information is available free of charge on the ACS Publications website at DOI: 10.1021/acs.est.8b07241.

Description of ULE implementation policy in China's power sector, location and technology details for ULE technologies at individual power plants, discussion on reliability of flue gas flow rate and pollution concentration measurements, and comparison of post-ULE emissions factors with the literature (PDF)

Supplementary Data File (XLSX)

■ AUTHOR INFORMATION

Corresponding Authors

*(A.Y.K.) Phone: +1-908-227-1880; e-mail: anthonyku@nicenergy.com.

*(J.L.) E-mail: linjt@pku.edu.cn.

ORCID

Anthony Y. Ku: 0000-0003-3762-2914

Notes

The authors declare no competing financial interest.

Emissions data are available upon request.

■ ACKNOWLEDGMENTS

The authors are grateful to Wenqiang Xu, Weidong Jiao, and Yonglong Li for helpful discussions. This research is supported in part by the National Natural Science Foundation of China (41775115).

■ REFERENCES

(1) Clean Air Alliance of China. State Council Air Pollution Prevention and Control Action Plan, Issue II, 2013, http://en.cleanairchina.org/product/6346.html (English translation).

(2) National Development and Reform Commission of China, Ministry of Environmental Protection of China, National Energy Administration of China. The Upgrade and Transformation Action Plan for Coal-Fired Power Energy Saving and Emission Reduction (2014−2020), 2014. http://www.gov.cn/gongbao/content/2015/content_2818468.htm.

(3) Ohara, T.; Akimoto, H.; Kurokawa, J.; Horii, N.; Yamaji, K.; Yan, X.; Hayasaka, T. An Asian emission inventory of anthropogenic emissions sources for the period 1980−2000. *Atmos. Chem. Phys.* **2007**, *7*, 4419−4444.

(4) Zhang, Q.; Streets, D. G.; Carmichael, G. R.; He, K. B.; Huo, H.; Kannari, A.; Klimont, Z.; Park, I. S.; Reddy, R.; Fu, J. S.; Chen, D.; Duan, L.; Lei, Y.; Wang, L. T.; Yao, Z. L. Asian emissions in 2006 for

DOI: 10.1021/acs.est.8b07241
Environ. Sci. Technol. 2019, 53, 2570−2578

the NASA INTEX-B mission. *Atmos. Chem. Phys.* **2009**, *9*, 5131−5153.
(5) Zhao, Y.; Wang, S.; Nielsen, C. P.; Li, X.; Hao, J. M. Establishment of a database of emission factors for atmospheric pollutants from Chinese Coal-fired power plants. *Atmos. Environ.* **2010**, *44*, 1515−1523.
(6) Tian, H. Z.; Liu, K. Y.; Hao, J. M.; Wang, Y.; Gao, J. J.; Qiu, P. P.; Zhu, C. Y. Nitrogen Oxides Emissions from Thermal Power Plants in China: Current Status and Future Predictions. *Environ. Sci. Technol.* **2013**, *47* (19), 11350−11357.
(7) Li, M.; Liu, H.; Geng, G.; Hong, C.; Liu, F.; Song, Y.; Tong, D.; Zheng, B.; Cui, H.; Man, H.; Zhang, Q.; He, K. B. Anthropogenic emission inventories in China: a review. *Natl. Sci. Rev.* **2017**, *4*, 834−866.
(8) Liu, F.; Zhang, Q.; Tong, D.; Zheng, B.; Li, M.; Huo, H.; He, K. B. High-resolution inventory of technologies, activities and emissions of coal-fired power plants in China from 1990 to 2010. *Atmos. Chem. Phys.* **2015**, *15*, 13299−13317.
(9) Ma, Z.; Deng, J.; Li, Z.; Li, Q.; Zhao, P.; Wang, L.; Sun, Y.; Zheng, H.; Pan, L.; Zhao, S.; Jiang, J.; Wang, S.; Duan, L. Characteristics of NOx emission from Chinese coal-fired power plants equipped with new technologies. *Atmos. Environ.* **2016**, *131*, 164−170.
(10) Wang, S. M.; Song, C.; Chen, Y.; Sun, P. Technology research and engineering applications of near-zero emission coal-fired power plants. *Res. Env. Sci.* **2015**, *28*, 487−494.
(11) Sui, Z.; Zhang, Y.; Peng, Y.; Norris, P.; Cao, Y.; Pan, W. P. Fine particulate matter emission and size distribution characteristics in an ultra-low emission power plant. *Fuel* **2016**, *185*, 863−871.
(12) Zhao, L.; Zhou, H. Particle removal efficiency analysis of WESP in an ultra-low emission power plant. *Proc. Chin. Soc. Electrical Eng.* **2016**, *36*, 468−473.
(13) Li, Z.; Jiang, J.; Ma, Z.; Wang, S.; Duan, L. Effect of selective catalytic reduction (SCR) on fine particulate emission from two coal-fired power plants in China. *Atmos. Environ.* **2015**, *120*, 227−233.
(14) Li, Z.; Jiang, J.; Ma, Z.; Fajardo, O. A.; Deng, J.; Duan, L. Influence of flue gas desulfurization (FGD) installations on emission characteristics of PM2.5 from coal-fired power plants equipped with selective catalytic reduction (SCR). *Environ. Pollut.* **2017**, *230*, 655−662.
(15) Sun, Y. L.; Du, W.; Wang, Q. Q.; Zhang, Q.; Chen, C.; Chen, Y.; Chen, Z. Y.; Fu, P. Q.; Wang, Z. F.; Gao, Z. Q.; Worsnop, D. R. Real-Time Characterization of Aerosol Particle Composition above the Urban Canopy in Beijing: Insights into the Interactions between the Atmospheric Boundary Layer and Aerosol Chemistry. *Environ. Sci. Technol.* **2015**, *49* (19), 11340−11347.
(16) Zheng, G. J.; Duan, F. K.; Ma, Y. L.; Zhang, Q.; Huang, T.; Kimoto, T.; Cheng, Y. F.; Su, H.; He, K. B. Episode-Based Evolution Pattern Analysis of Haze Pollution: Method Development and Results from Beijing, China. *Environ. Sci. Technol.* **2016**, *50* (9), 4632−4641.
(17) Wang, S. X.; Zhao, M.; Xing, J.; Wu, Y.; Zhou, Y.; Lei, Y.; He, K. B.; Fu, L. X.; Hao, J. M. Quantifying the Air Pollutants Emission Reduction during the 2008 Olympic Games in Beijing. *Environ. Sci. Technol.* **2010**, *44* (7), 2490−2496.
(18) Lin, J.-T.; McElroy, M. B.; Boersma, K. F. Constraint of anthropogenic NOx emissions in China from different sectors: a new methodology using multiple satellite retrievals. *Atmos. Chem. Phys.* **2010**, *10*, 63−78.
(19) Dong, Y. L.; Jiang, X.; Liang, Z. H.; Yuan, J. H. Coal power flexibility, energy efficiency and pollutant emissions implications in China: A plant-level analysis based on case units. *Resources, Conservation & Recycling* **2018**, *134*, 184−195.
(20) Liu, X.; Xu, Y.; Zeng, X.; Zhang, Y.; Xu, M.; Pan, S.; Zhang, K.; Li, L.; Gao, X. Field measurements on the emission and removal of PM2.5 from coal-fired power stations: 1. Case study for a 1000 MW ultrasupercritical utility boiler. *Energy Fuels* **2016**, *30*, 6547−6554.
(21) Kannari, A.; Tonooka, Y.; Baba, T.; Murano, K. Development of multiple-species 1 km x 1 km resolution hourly basis emissions inventory of Japan. *Atmos. Environ.* **2007**, *41*, 3428−3439.
(22) Protection of Environment. 75.10, General operating requirements. U.S. Code of Federal Regulations, Title 40, 2002. https://ecfr.io/Title-40/pt40.18.75.
(23) Abdel-Aziz, A.; Frey, H. C. Development of hourly probabilistic utility NOx emission inventories using time series techniques: Part I-Univariate approach. *Atmos. Environ.* **2003**, *37*, 5379−5389.
(24) Abdel-Aziz, A.; Frey, H. C. Development of hourly probabilistic utility NOx emission inventories using time series techniques: Part II-multivariate approach. *Atmos. Environ.* **2003**, *37*, 5391−5401.
(25) China Electric Power Enterprise Association. *Compilation of Information on China Electric Power Industry 2015*; China Electric Power Enterprise Association: Beijing, 2016.
(26) Ministry of Environmental Protection of China. *General Administration of Quality Supervision. Emissions Standard of Air Pollutants for Thermal Power Plants*, No. GB/T 13223−2011, July, 29, 2011.
(27) Hoesly, R. M.; Smith, S.; Feng, L.; Klimont, Z.; Janssens-Maenhout, G.; Pitkanen, T.; Seibert, J. J.; Vu, L.; Andres, R. J.; Bolt, R. M.; Bond, T. C. Historical (1750−2014) anthropogenic emissions of reactive gases and aerosols from the Community Emission Data System (CEDS). *Geosci. Model Dev. Discuss.* **2018**, *11*, 369−408.
(28) Zhang, L.; Zhao, T.; Gong, S.; Kong, S.; Tang, L.; Liu, D.; Wang, Y.; Jin, L.; Shan, Y.; Tan, C.; Zhang, Y.; Guo, X. Updated emission inventories of power plants in simulating air quality during haze periods over East China. *Atmos. Chem. Phys.* **2018**, *18*, 2065−2079.

DOI: 10.1021/acs.est.8b07241
Environ. Sci. Technol. 2019, 53, 2570−2578